Nuclear Inst. and Methods in Physics Research B 436 (2018) 68–73

Contents lists available at ScienceDirect

Nuclear Inst. and Methods in Physics Research B

journal homepage: www.elsevier.com/locate/nimb

Implementation of photon elastic scattering in GEANT4

G.V. Turturica[a,b], V. Iancu[a,*], G. Suliman[a], C.A. Ur[a,b,*]

[a] Extreme Light Infrastructure-Nuclear Physics/Horia Hulubei National Institute for R&D in Physics and Nuclear Engineering, 30 Reactorului Street, P.O.B. MG-6, Bucharest-Magurele, Judet Ilfov RO-077125, Romania
[b] Politehnica University of Bucharest, Bucharest, Romania

ARTICLE INFO

Keywords:
Elastic scattering
Delbrück scattering
Rayleigh scattering
GDR
GEANT4

ABSTRACT

A complete theoretical framework for photon elastic scattering has been implemented in GEANT4 and is validated against experimental results. The implementation covers all atomic numbers and energy range between 0.3 MeV and 20 MeV. The total elastic scattering cross section is calculated based on scattering amplitudes to account for interferences between coherent processes. New scattering amplitudes are calculated for Rayleigh scattering to extend the cross section data table and avoid interpolation and extrapolation. Validation on a significant number of test cases showed good agreement between our implementation and experimental data.

1. Introduction

The elastic scattering of photons has been a topic of interest in theoretical and experimental physics in the past century but it was mostly disregarded in the last two decades. The emergence of high-energy, high-flux laser Compton scattering (LCS) gamma sources, such as HIγS [1] and NewSubaru [2] as well as the future ELI-NP Gamma Beam System (GBS) [3] and SLEGS [4], brings the elastic scattering back into the focus of scientific research. The improved characteristics in terms of intensity and bandwith of LCS beams open the possibility to study such phenomena with unprecedented accuracy. Experimental proposals regarding more precise measurements of Delbrück scattering have already been put forward [5]. Elastic scattering is a source of background that becomes significant when using narrow bandwidth LCS beams for fundamental as well as applicative studies. For instance nuclear resonance fluorescence (NRF) for active interrogations of special nuclear materials is advantageous when performed with an LCS gamma beam, provided that a correct estimation of the elastic scattering background is undertaken [6].

Elastic scattering implementations from typical particle transport codes, such as GEANT4 [7] or MCNP [8], are limited to Rayleigh scattering and ignore the rest of the processes [9]. This approximation is suited for low photon energies but yields a considerable difference between simulation and experiment for energies above 1 MeV. Only recently, Omer and Hajima [10] made the first attempt at implementing the total elastic scattering cross section in GEANT4. However, the implementation was limited to a maximum photon energy of 3 MeV. Here, we extend the implementation of photon elastic scattering for energies up to 20 MeV to cover the energy domain of the future LCS source at ELI-NP facility. Hence the future photonuclear experiments and applications at ELI-NP and other similar facilities can benefit from a correct estimation of elastic scattering background [11,12]. Our implementation uses the complete theoretical framework for the photon elastic scattering. The total elastic scattering cross section is calculated based on scattering amplitudes to account for the constructive and destructive interference effects between the coherent processes. In order to fully describe the elastic scattering of photons the following processes have been considered: Rayleigh, nuclear Thomson, Delbrück and nuclear resonance scattering. Rayleigh scattering amplitudes were calculated using the second-order scattering matrix (S-matrix) and modified form factors. Delbrück scattering contribution was implemented using scattering amplitudes based on first order Born approximation. Nuclear Thomson scattering and nuclear resonance scattering contributions were calculated using analytical formulas. Section 2 presents the theoretical background for the four components of the elastic scattering process. Data processing and code implementation are described in Section 3. Verification, validation procedures and results discussion follow in Section 4.

2. Theoretical background

The differential cross section for elastic scattering consists of two terms and can be expressed as [13]:

* Corresponding author at: Extreme Light Infrastructure-Nuclear Physics/Horia Hulubei National Institute for R&D in Physics and Nuclear Engineering, 30 Reactorului Street, P.O.B. MG-6, Bucharest-Magurele, Judet Ilfov RO-077125, Romania (V. Iancu, C.A. Ur).
E-mail addresses: violeta.iancu@eli-np.ro (V. Iancu), calin.ur@eli-np.ro (C.A. Ur).

https://doi.org/10.1016/j.nimb.2018.09.007
Received 18 May 2018; Received in revised form 4 September 2018; Accepted 4 September 2018
Available online 13 September 2018
0168-583X/

$$\left(\frac{d\sigma}{d\Omega}\right)^{exp} = \left(\frac{d\sigma}{d\Omega}\right)^{coh} + \left(\frac{d\sigma}{d\Omega}\right)^{incoh} \quad (1)$$

where *coh* and *incoh* refers to the coherent and incoherent part of the elastic scattering cross section.

2.1. Coherent scattering cross section

The coherent term in Eq. (1) can be calculated as:

$$\left(\frac{d\sigma}{d\Omega}\right)^{coh} = \frac{1}{2}(|A_{\parallel}|^2 + |A_{\perp}|^2) \quad (2)$$

where $A_{\parallel}$ and $A_{\perp}$ are the scattering amplitudes parallel and perpendicular to the scattering plane. The scattering amplitudes are calculated according to the relation:

$$A = A^T + A^R + A^D + A^N \quad (3)$$

where indexes refer to the nuclear Thomson (T), Rayleigh (R), Delbrück (D) and nuclear resonance scattering (N).

2.1.1. Nuclear Thomson scattering

Nuclear Thomson scattering amplitudes can be calculated analytically using the following expressions [14]:

$$A_{\perp} = -r_e Z^2 \frac{m_e}{M} \quad (4)$$

$$A_{\parallel} = -r_e Z^2 \frac{m_e}{M} cos(\theta) \quad (5)$$

where r_e is the classical electron radius, m_e is the electron mass, Z is the atomic number, M is the nucleus mass and θ is the scattering angle. Nuclear Thomson amplitudes are energy independent and have no imaginary part. The angular distribution is contained in $A_{\parallel}$ in the form of cos(θ).

2.1.2. Rayleigh scattering

Rayleigh scattering can be understood as the scattering of an electromagnetic wave off the bound atomic electrons in a collective and coherent fashion. The atom as a whole recoils in order to achieve conservation of momentum. A rigorous theoretical description of the process would require taking into account the contribution of each electron to the scattering process but this can become computing intensive [14]. As a result two approximate methods were used to calculate Rayleigh scattering amplitudes. The first method is based on Thomson amplitudes and atomic form factors [14], while the second method takes into account the individual contribution of the significant electrons and a general description for the rest of them [15,16].

In the first method the scattering amplitudes are calculated according to:

$$A_{\perp} = \underbrace{\underbrace{-r_e}_{\text{Thomson}} f\left(x, Z\right)}_{\text{Rayleigh}} \quad (6)$$

$$A_{\parallel} = \underbrace{\underbrace{-r_e cos(\theta) f}_{\text{Thomson}}\left(x, Z\right)}_{\text{Rayleigh}} \quad (7)$$

where f(x, Z) is the atomic form factor representing the electronic charge distribution. The form factor is a function of Z and the momentum transfer x:

$$x = \frac{\sin(\theta/2)}{\lambda} \quad (8)$$

with λ the photon wavelength (in angstroms). Multiple types of form factors have been proposed in previous studies: non-relativistic, relativistic, modified and anomalous, and their validity was studied by Kissel et al. [17]. Tabulated values of form factors are found in literature for different ranges of x and Z values, e.g. Hubbell et al. made available complete form factor tables for a large range of x values [18,19]. The form factor approach gives satisfactory results for low-energy photons and for low Z scatterers but deviates from experimental results when high energy and high Z elements are concerned. Currently the most precise calculations of the Rayleigh scattering amplitudes based on form factors can be obtained using modified form factors coupled with anomalous corrections [17].

The second method used to obtain Rayleigh scattering amplitudes is based on numerical calculations of second-order scattering matrix [15,16]. The S-matrix formalism gives the best results but it is computationally demanding. Kissel et al. [14] developed a simplified method to accurately generate Rayleigh scattering amplitudes using S-matrix calculations for the inner-shell electrons, which accounts for most of the contribution, and form-factor-based amplitudes for the outer electrons. The results of this method reproduce more accurately the experimental data, compared to the form factor approach [17]. Data tables of scattering amplitudes obtained with the use of S-matrix calculations can be found in the Rayleigh scattering database (RTAB) [20] for photons up to 2.754 MeV.

2.1.3. Delbrück scattering

Delbrück scattering is understood as virtual pair production in the nuclear field followed by annihilation with the emission of a single photon [21]. Delbrück scattering amplitudes, up to 100 MeV, were calculated using first-order Born approximation, and tabulated by Falkenberg et al. [22]. For the limiting case of forward scattering, analytical formulas may be employed to obtain zero degree scattering amplitudes [23].

Comparison between experimental and theoretical data for high Z numbers shows the limitations of the first-order Born approximation due to exclusion of multiphoton exchange with differences up to 40 % [24,25]. For a better agreement between experimental and theoretical results, Coulomb corrections have to be applied. Multiple authors proposed empirical [26,27] and theoretical [24,25] formulations for the Coulomb corrections, with limited progress on the theoretical side.

The general properties of the Coulomb corrections were inferred from experimental data and were shown to be small for scatterers with $Z < 50$, i.e. the accuracy of the Born approximation is within 5 % below $Z = 50$ [21]. These corrections are also dependent on the photon energy and the scattering angle. Below 4 MeV, the corrections add up to the Delbrück scattering amplitudes; between 4 and 7 MeV the corrections seem to have a negligible effect to the total cross sections, while above 7 MeV, there seems to be a significant contribution but with an opposite sign with respect to the low energy part [26]. The angular dependence of the Coulomb corrections follows a similar pattern as the lowest order approximation, showing a fast decay from low angles to an almost constant value at angles above 90° [26,27].

2.1.4. Nuclear resonance scattering

Nuclear resonance scattering is referred to the scattering off the tail of the giant-dipole-resonance (GDR). This process contributes to the coherent scattering cross section and also to the incoherent scattering cross section. In this region the photonuclear absorption cross section can be approximated using one or two Lorentzian lines. Scattering amplitudes can be calculated using the optical theorem and dispersion relations [21]:

$$A_{\perp}^N = \frac{E^2}{4\pi\hbar c r_e} \sum_{\nu=1}^{2} \sigma_\nu \Gamma_\nu \frac{(E_\nu^2 - E^2 + iE\Gamma_\nu)}{(E_\nu^2 - E^2)^2 + E^2\Gamma_\nu^2} \quad (9)$$

$$A_{\parallel}^N = A_{\perp}^N \cos(\theta) \quad (10)$$

where E is the photon energy and E_ν, Γ_ν, σ_ν are the GDR parameters with ν the Lorentzian line index. The imaginary part of Eq. (9) yields a

contribution only above the (γ,n) threshold and it is set to zero below. The angular contribution to the scattering amplitude is accounted for by the cos(θ) of the parallel amplitude. Tabulated experimental values of the GDR parameters are found in literature [28,29] for a wide range of Z and A values. Besides the GDR parameters, the (γ,n) separation threshold values are needed to calculate the imaginary part of the scattering amplitude.

2.2. Incoherent scattering cross section

The incoherent part of Eq. (1) corresponds to the transfer of two angular momentum units in the nuclear resonance scattering process [30]. The cross section for this interaction can be obtained using [31]:

$$\left(\frac{d\sigma}{d\Omega}\right)^{inc} = r_e^2 (I_0 K_0 20 | I_0 2 I_0 K_0)^2 [(2\alpha_1 - \alpha_2)^2 + (2\beta_1 - \beta_2)^2] \frac{1}{40} (13 + cos^2(\theta)) \tag{11}$$

where I_0 is the nuclear spin, K_0 is the projection of I_0 on the symmetry axis of the nucleus, α_1, α_2, β_1 and β_2 can be obtained from:

$$A_{\perp}^{N} = \sum_{\nu=1}^{2} (\alpha_\nu + i\beta_\nu) \tag{12}$$

where $A_{\perp}^{N}$ is the perpendicular scattering amplitude of the coherent part of the nuclear resonance scattering.

The contribution of the incoherent part to the total cross section can be relatively small below 7 MeV [30] but gets noticeable around the minimum of the elastic scattering cross section. The incoherent scattering cross section contribution to the total differential cross section vanishes for nuclei where $I_0 < 1$.

3. GEANT4 implementation of photon elastic scattering

Here we describe the implementation of a complete theoretical framework for photon elastic scattering cross section for an energy range between 0.3 MeV and 20 MeV.

In order to implement the elastic scattering a new class named ElasticScatteringModel was created. The class inherits from G4VEmModel same as G4PenelopeRayleighModel or G4KleinNishinaModel. Three functions were overwritten from the standard implementation, namely: *Initialize* — the function in charge of the initialization of the process — *ComputeCrossSectionPerAtom* — the method to compute the cross section depending on a particular atom — and *SampleSecondaries* — the function in charge of the sampling procedures for the secondary particles.

In the initialization phase *Initialize* is called in order to construct a three dimensional table of elastic scattering cross sections. Here, the code retrieves/computes all scattering amplitudes for each elastic process and subsequently calculates the elastic scattering cross section by summing the coherent scattering cross section using Eqs. (2) and (3) with the incoherent scattering cross section calculated with Eq. (11). The density of the grid is user controlled and defines the resolution of the calculated cross sections. The calculated cross sections for all the isotopes used in the geometrical implementation are stored as a function of the photon energy and the scattering angle. Five additional functions were created in order to calculate the individual contributions to the total elastic scattering cross section.

Nuclear Thomson amplitudes were calculated based on the analytical formulas presented in Section (2.1.1). Given the continuous form of the data no interpolation procedures were necessary.

The Rayleigh scattering amplitudes are computed using the S-matrix method up to 6 MeV and using modified form factors from 6 MeV up to 20 MeV. Up to 6 MeV we have computed the scattering amplitudes using the code developed by Kissel to create the RTAB database [14,20]. Access to the code allowed us to increase the grid density and to extend the database up to 6 MeV. Due to code limitations [32], for photons with energy higher than 6 MeV, the scattering amplitudes were computed using the form factor approach based on modified form factors. The modified form factors were obtained as described in reference [20].

Delbrück amplitudes were taken from Falkenberg's tabulations [22]. The available data covers photon energies from 0.255 MeV up to 100 MeV. The amplitudes provided do not cover a fixed grid of scattering angles. The low energy part, up to 3 MeV, covers at least the angles from 10 to 150°, while the high energy part has a fixed grid between 1 and 120°. The zero degree amplitudes were calculated based on analytical formulas [23]. In order to complete a two dimensional grid, as a function of energy and θ, interpolation and extrapolation procedures were employed.

Coherent nuclear resonance scattering amplitudes were calculated using the Eqs. (9) and (10). The GDR parameters were extracted form the RIPL-3 database [29] and the neutron separation thresholds were obtained from NUDAT [33].

To compute the incoherent nuclear resonance scattering cross sections we used the input data for the coherent nuclear resonance amplitudes. The GDR parameters, neutron separation thresholds, the nuclear spin and the projection of the states were obtained from the RIPL-3 database [29].

The angular distribution of the scattered photon is sampled from the differential cross section using a modified version of the TH1::GetRandom function, part of ROOT [34]. The azimuthal angle ϕ is sampled from a uniform random distribution. The average sampling time of the current implementation is similar to the sampling time of G4PenelopeRayleigh.

4. Results and discussions

To verify and validate the implementation we performed simulations using GEANT4, version 10.2.2, for several test cases. We tested the agreement between theory, simulation and experimental data by comparing the simulated angular distribution, energy distribution and atomic number distribution of elastically scattered γ-rays with theory and experimental results. The simulation geometry was kept as simple as possible containing a mono-energetic point-like source, which generates a beam of photons along the z-direction and a scattering target that was a cube of 0.01 cm side made of the studied material. The scattered photon counting was done on a surface defined by the polar angle θ with $\Delta\theta = 0.5°$ and the entire azimuthal angle ϕ. The angular distribution was mapped using a 5° grid on theta. The simulated cross section was calculated using the number of incident and scattered photons, the target parameters and the solid angle of the counter. The newly implemented elastic scattering process was the only physical process active in order to ease the computational effort. For the test simulations we used an uniform grid of 181 × 1000 points (angle versus energy).

In the first part of the validation, low energy photon scattering on ^{238}U was simulated and compared with data presented by Milstein and Schumacher [35]. The simulated curves shown in Fig. 1, are in good agreement with the experimental points for energies below 1.3 MeV. Significant differences between the simulated and experimental cross sections are observed at 2.754 MeV. The observed disagreement is attributed to the lack of Coulomb corrections [35] in the current implementation.

Fig. 2 illustrates the atomic number dependence of the differential cross section of 2.754 MeV photons elastically scattered at various angles. Note that overall there is good agreement between the experimental and simulated results except for small scattering angles and high Z materials where the Coulomb corrections play an important role [27]. Indirectly, the graph highlights the variation of the Coulomb correction terms with respect to atomic number and scattering angle for a fixed photon energy of 2.754 MeV. For scattering angles larger than 90° the Coulomb corrections effect is insignificant, regardless of the atomic number.

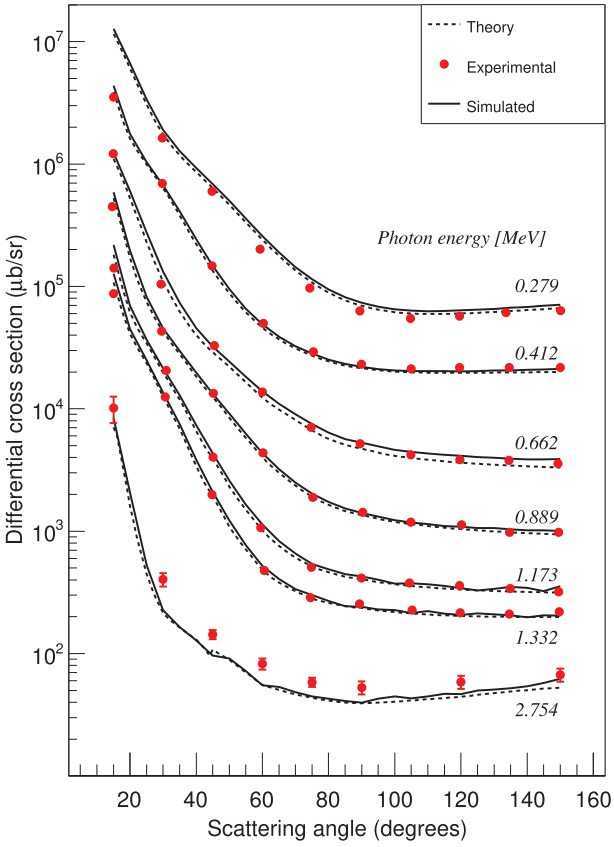

Fig. 1. Elastic scattering differential cross section (μb/sr) versus scattering angle (degrees) for ^{238}U for various photon energies. The solid lines represent a linear interpolation of simulated points obtained using the current implementation. The dashed lines represent the theoretical data used for the current implementation. The full circles (red) are experimental points obtained from Milstein and Schumacher [35]. (For interpretation of the references to colour in this figure legend, the reader is referred to the web version of this article.)

To test the performance of the simulation for high energy photons we use ^{238}U as a test case to compare the simulated results with the experimental data provided by Rullhusen et al. [26] for 8.998 MeV photons. Fig. 3 shows the elastic scattering cross section as a function of the scattering angle for photons of 8.998 MeV. In this energy region there are two main factors that will limit the accuracy of our current implementation, Coulomb corrections for Delbrück scattering, and the uncertainties in the GDR parameters. For angles below 90° Delbrück scattering contributes considerably to the total cross section which explains the discrepancies between the simulated and the experimental data at forward angles.

At high energies the interference between nuclear Thomson and nuclear resonance scattering amplitudes gives the largest contribution to the elastic scattering for scattering angles above 90°. Given the simple description of nuclear Thomson, the GDR parameters will solely determine the accuracy of the calculations. In this energy region sizable discrepancies between experimental data and theory have been reported [26], suggesting a sensitive correlation between elastic scattering cross section and the GDR parameters. The simulation results presented in Fig. 3 used GDR parameters obtained from RIPL-3 database [29] and show good agreement with the experimental data for angles above 90°, which is the angular interval of interest for experiments at ELI-NP GBS.

Fig. 4 shows the results of another test case up to a photon energy of 20 MeV. Experimental data for ^{197}Au [36] at a fixed scattering angle of 135° is compared with theoretical cross sections and simulated results.

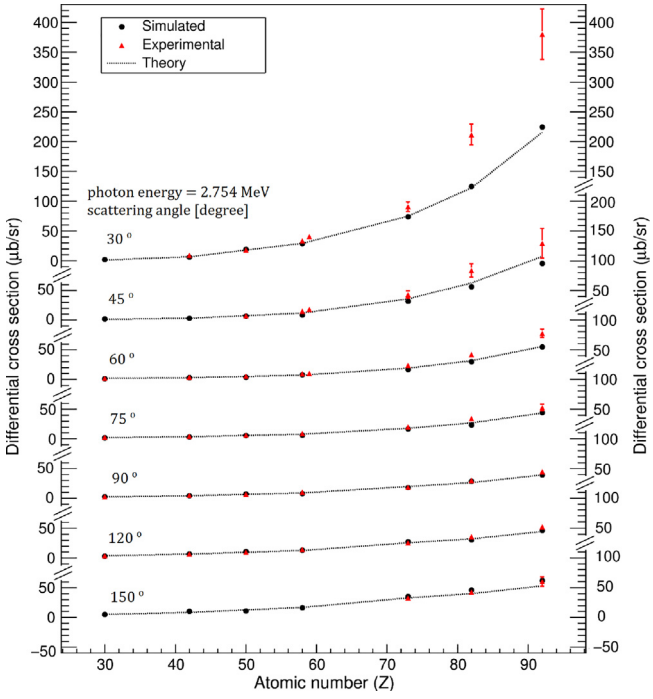

Fig. 2. Elastic scattering differential cross section (μb/sr) versus atomic number for a fixed photon energy of 2.754 MeV. The full circles (black) represent the simulated points obtained using the current implementation. The dotted lines represent the theoretical data used for the current implementation. The triangle markers (red) are experimental points obtained from Milstein and Schumacher [35]. (For interpretation of the references to colour in this figure legend, the reader is referred to the web version of this article.)

Simulated data was obtained using slightly modified GDR parameters from Fuller and Weiss [37] where a 0.8 factor was applied to the cross section of the second Lorentzian. The agreement between experimental and simulated data is vastly improved by using the modified deformed parameters instead of the spherical ones from RIPL-3.

An indication of the improvement in the modeling of the photon elastic scattering obtained with the current implementation with regard to the default GEANT4 implementation can be observed in Fig. 5. This graph presents a comparison between simulated and experimental data for U^{238} at 120° for the 0.2–12 MeV energy interval. The simulated points were obtained in two different configurations. The full circles (black) represent simulated results using the elastic scattering implementation presented in this work. The blue squares show simulated data obtained by using the available implementation of photon elastic scattering, implementation that contains only Rayleigh scattering (G4PenelopeRayleigh). As expected, the low energy part of the graph is reproduced well by both implementations however, differences between the two implementations start to appear at energies above 1 MeV and become significant at high energies. The large scattering angle, i.e. limited contribution of the Coulomb corrections, and proper GDR parameters (Fig. 3) yield very good agreement between our implementation and the experimental data [30], which is clearly observed in Fig. 5.

5. Conclusions

This work presents the GEANT4 implementation of the photon elastic scattering up to photon energies of 20 MeV. A complete theoretical framework was used in order to account for the interference effects between the processes involved in this interaction. Validation procedures employed for a significant number of test cases showed good agreement between the experimentally measured and simulated cross sections. The current modeling of the photon elastic scattering

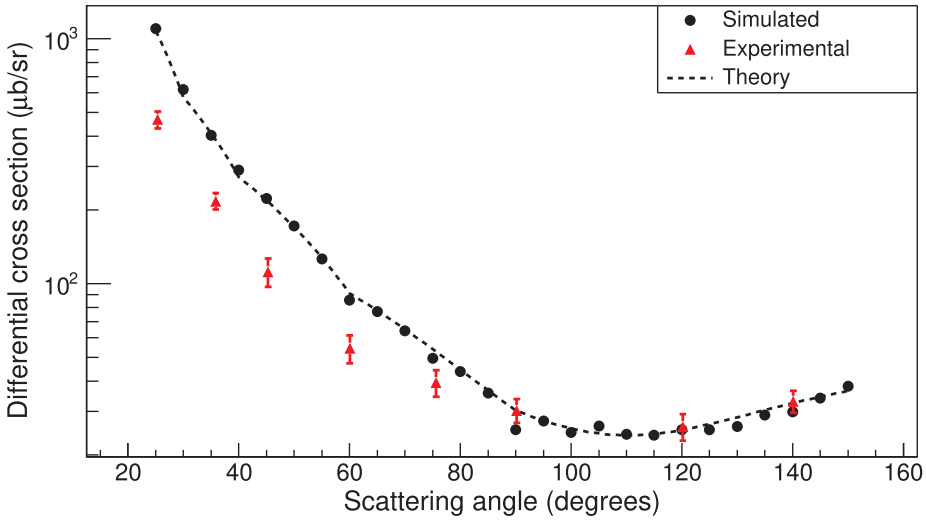

Fig. 3. Elastic scattering differential cross section (μb/sr) versus scattering angle (degrees) for ^{238}U at a fixed photon energy of 8.998 MeV. Simulated data obtained by using the current implementation is represented by full circles (black). The dashed line represents the theoretical data used for the current implementation. The triangle markers (red) are experimental points obtained from Rullhusen et al. [26]. (For interpretation of the references to colour in this figure legend, the reader is referred to the web version of this article.)

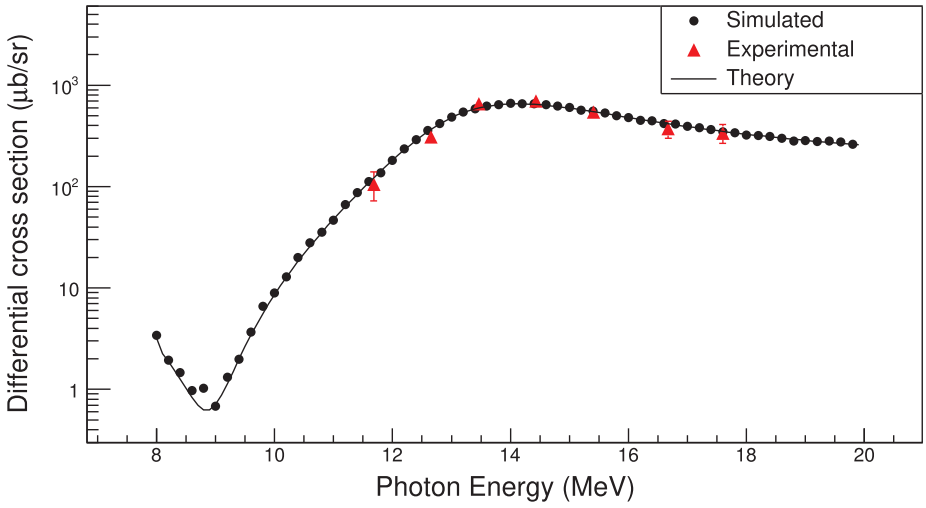

Fig. 4. Elastic scattering differential cross section (μb/sr) versus photon energy (MeV) for ^{197}Au at a fixed scattering angle of 135°. The full circles (black) represent simulated points obtained by using the current implementation. The continuous line represents the theoretical data used for the current implementation. The triangle markers (red) are experimental points obtained from O'Connel et al. [36]. (For interpretation of the references to colour in this figure legend, the reader is referred to the web version of this article.)

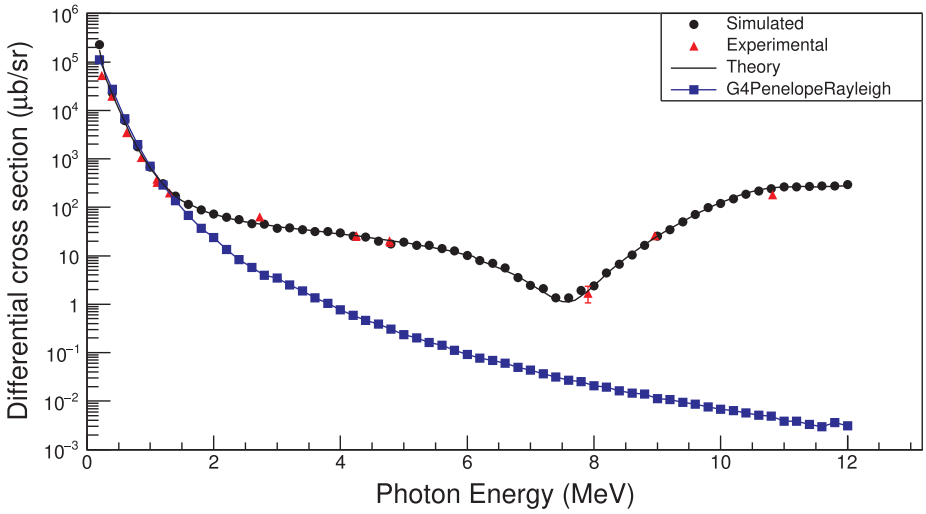

Fig. 5. Elastic scattering differential cross section (μb/sr) versus photon energy (MeV) for ^{238}U at a fixed scattering angle of 120°. The full circles (black) are simulated points obtained from the current implementation. The continuous line (black) represents the theoretical data used for the current implementation. The square markers (blue) are simulated points obtained using G4PenelopeRayleigh. The triangle markers (red) are experimental points obtained from Schumacher et al. [30]. (For interpretation of the references to colour in this figure legend, the reader is referred to the web version of this article.)

best reproduces the experimental data at scattering angles larger than 90°, which is the angular domain of interest in the detection of NRF rays for fundamental nuclear physics as well as for the NRF-based applications. Considerable improvements in accuracy for forward scattering angles can be achieved including higher orders for Delbrück scattering.

Acknowledgments

We would like to thank Dr. Lynn Kissel for providing the code needed to calculate Rayleigh scattering amplitudes and for his guidance and advice in using the code. We thank D. Gambacurta and Y. Xu for very useful discussions. The Extreme Light Infrastructure – Nuclear

Physics project is co-financed by the Romanian Government and the European Union through the Regional Development Fund.

References

[1] H.R. Weller, M.W. Ahmed, H. Gao, W. Tornow, Y.K. Wu, M. Gai, R. Miskimen, Research opportunities at the upgraded HIγS facility, Prog. Part. Nucl. Phys. 62 (2009) 257–303.

[2] S. Miyamoto, S. Amano, S. Hashimoto, N. Sakai, A. Koizumi, T. Hashimoto, T. Shizuma, H. Utsunomiya, T. Yamagata, H. Akimune, T. Shima, D. Li, Y. Asano, H. Ohkuma, Laser compton scattering gamma-ray beam source at NewSUBARU storage ring, Nucl. Phys. Gamma-Ray Sources Nucl. Security Nonproliferation (2014) 143–150.

[3] O. Adriani, et al., Technical design report, EuroGammaS proposal for the ELI-NP Gamma Beam System doi:arXiv:1407.3669v1.

[4] Q.Y. Pan, W. Xu, W. Luo, X.Z. Cai, J.G. Chen, G.T. Fan, G.W. Fan, W. Guo, Y.J. Li, G.Q. Lin, Y.G. Ma, W.Q. Shen, X.C. Shi, H.W. Wang, B.J. Xu, J.Q. Xu, Y. Xu, Z. Yan, L.F. Yang, M.H. Zhao, A future laser compton scattering (LCS) γ-ray source: SLEGS at SSRF, Synch. Rad. News 22 (3) (2009) 11.

[5] J.K. Koga, T. Hayakawa, Possible precise measurements of Delbrück scattering using polarized photon beams, Phys. Rev. Lett 118 (2017) 204801.

[6] B.A. Ludewigt, B.J. Quiter, S.D. Ambers, Nuclear Resonance Fluorescence for Safeguards Applications, DOE report (2011).

[7] S. Agostinelli, et al., GEANT4 – a simulation toolkit, Nucl. Instr. and Meth. A 506 (2003) 250–303.

[8] X-5 Monte-Carlo Team, MCNP – A General N-Particle Transport Code - LA-UR-03-1987 (2003).

[9] M. Batic, G. Hoff, M. Pia, P. Saracco, Photon elastic scattering simulation: validation and improvements to GEANT4, IEEE Trans. Nucl. Sci 59 (2012) 1636–1664.

[10] M. Omer, R. Hajima, Including Delbrück scattering in GEANT4, Nucl. Instr. and Meth. B 405 (2017) 43–49.

[11] C.A. Ur, A. Zilges, N. Pietralla, J. Beller, B. Boisdeffre, M.O. Cernaianu, V. Derya, B. Loher, C. Matei, G. Pascovici, C. Petcu, C. Romig, D. Savran, G. Suliman, E. Udup, V. Werner, Nuclear resonance fluorescence experiments at ELI-NP, Rom. Rep. Phys. 68 (2016) S483–S538.

[12] G. Suliman, V. Iancu, C.A. Ur, M. Iovea, I. Daito, H. Ohgaki, Gamma-beam industrial applications at ELI-NP, Rom. Rep. Phys. 68 (2016) S799–S845.

[13] M. Schumacher, F. Smend, W. Mückenheim, P. Rullhusen, H.G. Börner, Nuclear photoexcitation and Delbrück scattering studied in the energy range 2–8 MeV, Z. Phys. A 300 (1981) 193–203.

[14] L. Kissel, R.H. Pratt, B. Crasemann (Eds.), Atomic Inner-Shell Physics, Plenum Press, New York, 1956.

[15] L. Kissel, R.H. Pratt, New predictions for rayleigh scattering: 10 keV–10 MeV, Phys. Rev. Lett. 40 (1978) 387.

[16] W.R. Johnson, K. Cheng, Elastic scattering of 0.1–1 MeV photons, Phys. Rev. A 13 (2) (1976) 692.

[17] L. Kissel, B. Zhou, S.C. Roy, S.K.S. Gupta, R.H. Pratt, The validity of form-factor, modified-form-factor and anomalous-scattering-factor aproximations in elastic scattering calculations, Acta Cryst. A 51 (1995) 271–288.

[18] J.H. Hubbell, W.J. Veigele, E.A. Briggs, R.T. Brown, D.T. Cromer, Atomic form factors, incoherent scattering functions, and photon scattering cross section, J. Phys. Chem. Ref. Data 4 (1975) 471.

[19] J.H. Hubbell, I. Øverbø, Relativistic atomic form factors and photon coherent scattering cross sections, J. Phys. Chem. Ref. Data 8 (1979) 69.

[20] L. Kissel, RTAB: the Rayleigh scattering database, Rad. Phys. Chem. 59 (2000) 185–200.

[21] P. Rullhusen, W. Mücknheim, F. Smend, M. Schumacher, G.P.A. Berg, K. Mork, L. Kissel, Test of vacuum polarization by precise investigation of Delbrück scattering, Phys. Rev. C 23 (4) (1981) 1375.

[22] H. Falkenberg, A. Hünger, P. Rullhusen, M. Schumacher, A.I. Milstein, K. Mork, Amplitudes for Delbrück scattering, Atom. Data Nucl. Data 50 (1992) 1–27.

[23] E.M.A. Hussein, Radiation Mechanics, Principles and Practice, Elsevier, 2007.

[24] A. Scherdin, A. Schäfer, W. Greiner, G. Soff, P.J. Mohr, Coulomb corrections to Delbrück scattering, Z. Phys. A 353 (1995) 273–277.

[25] A. Scherdin, A. Schäfer, W. Greiner, G. Soff, Delbrück scattering in a strong external field, Phys. Rev. D 45 (8) (1992) 2982–2987.

[26] P. Rullhusen, U. Zurmühl, F. Smend, M. Schumacher, H.G. Börner, S.A. Kerr, Giant dipole resonances and Coulomb correction effect in Delbrück scattering studied by elastic and Raman scattering of 8.5 to 11.4 MeV photons, Phys. Rev. C 27 (2) (1983) 559.

[27] B. Kasten, D. Schaupp, P. Rullhusen, F. Smend, M. Schumacher, L. Kissel, Coulomb correction effect in Delbrück scattering and atomic Rayleigh scattering of 1–4 MeV photons, Phys. Rev. C 33 (5) (1986) 1606.

[28] V.A. Plujko, R. Capote, O.M. Gorbachenko, Giant dipole resonance parameters with uncertainties from photonuclear cross sections, Atom. Data Nucl. Data 97 (2011) 567–585.

[29] R. Capote, M. Herman, P. Oblozinsky, P.G. Young, S. Goriely, T. Belgya, A.V. Ignatyuk, A.J. Koning, S. Hilaire, V.A. Plujko, M. Avrigeanu, O. Bersillon, M.B. Chadwick, T. Fukahori, Z. Ge, Y. Han, S. Kailas, J. Kopecky, V.M. Maslov, G. Reffo, M. Sin, E.S. Soukhovitskii, P. Talou, Reference input parameter library (RIPL-3), Nucl. Data Sheets 110 (12) (2009) 3107–3214.

[30] M. Schumacher, P. Rullhusen, F. Smend, W. Mücknheim, H.G. Börner, The energy dependence of Delbrück scattering investigated at Z = 73, 82 and 92, Nucl. Phys. A 346 (1980) 418–430.

[31] E.G. Fuller, E. Hayward, The nuclear photoeffect in Holmium and Erbium, Nucl. Phys. 30 (1962) 613–635.

[32] We limited the S-matrix calculations at 6 MeV due to data overflow problems.

[33] R. Kinsey, et al., The NUDAT/PCNUDAT Program for Nuclear Data, paper submited to the 9th International Symposium of Capture Gamma-ray Spectroscopy and Related Topics (1996).

[34] R. Brun, F. Rademakers, ROOT – an object oriented data analysis framework, Nucl. Instr. and Meth. A 389 (1997) 81–86.

[35] A.I. Milstein, M. Schumacher, Present status of Delbrück scattering, Phys. Rep. 243 (1994) 183–214.

[36] J.S. O'Connel, P.A. Tipler, P. Axel, Elastic scattering of 11–17.7 MeV photons by Au measured with bremsstrahlung monochromator, Phys. Rev. 126 (1) (1962) 228–239.

[37] E.G. Fuller, M.S. Weiss, Splitting of the giant resonance for deformed nuclei, Phys. Rev. 112 (2) (1958) 560–567.